Effect of butadiene/styrene ratio, block structure and carbon nanotube content on the mechanical and electrical properties of thermoplastic elastomers after UV ageing

P. Costa [a, 1], S. Ribeiro [a, 1], G. Botelho [b], A.V. Machado [c], S. Lanceros Mendez [a, *]

[a] Centro/Departamento de Física, Universidade do Minho, 4710-057, Braga, Portugal

[b] Centro/Departamento de Química, Universidade do Minho, 4710-057, Braga, Portugal

[c] Institute for Polymer and Composites/I3N, Universidade do Minho, 4800-058, Guimarães, Portugal

Keywords:

Polymer photodegradation
TPE
CNT composites
Polymer chain scission
Cytotoxicity

Abstract

Thermoplastic elastomers based on a triblock copolymer styrene-butadiene-styrene (SBS) with different butadiene/styrene ratios, block structure and carbon nanotube (CNT) content were submitted to accelerated weathering in a Xenontest, in order to evaluate their stability to UV ageing. It was concluded that ageing mainly depends on butadiene/styrene ratio and block structure, with radial block structures exhibiting faster ageing than linear block structures. Moreover, the presence of carbon nanotubes in the SBS copolymer slows down the ageing of the copolymer. The evaluation of the influence of ageing on the mechanical and electrical properties demonstrates that the mechanical degradation is higher for the C401 sample, which is the SBS sample with the largest butadiene content and a radial block structure. On the other hand, a copolymer derivative from SBS, the styrene-ethylene/butadiene-

styrene (SEBS) sample, retains a maximum deformation of ~ 1000% after 80 h of accelerated ageing. The hydrophobicity of the samples decreases with increasing ageing time, the effect being larger for the samples with higher butadiene content. It is also verified that cytotoxicity increases with increasing UV ageing, with the exception of SEBS, which remains non-cytotoxic up to 80 h of accelerated ageing time, demonstrating its potential for applications involving exposure to the environment.

Introduction

Atmospheric conditions such as ultraviolet radiation, temperature, moisture, rain and pollutants have an important influence on the degradation of many polymers, being responsible for premature mechanical or electrical failure and hindering long term applications of several polymeric materials [1].

Thermoplastic elastomers (TPE) combine the mechanical properties of rubbers, such as high deformation and fast response time, with the processability and recyclability of thermoplastics [2,3]. Thermoplastic elastomers based on a triblock copolymer styrene-butadiene-styrene (SBS) do not require vulcanization, and show similar properties to rubbers. They show good chemical stability, low temperature flexibility and damping properties [4]. Several properties of these materials, including the electrical and mechanical ones, can be tailored by the addition of conductive fillers such as carbon nanoallotropes [5] in order to improve functionality and to extend their application range. Carbon nanotubes (CNT) as conductive filler for the development of polymer composites provide superior mechanical and electrical properties when compared to others nanoparticles [6,7]. Thus, composites using TPE as matrix and CNT as conductive material are being widely studied for sensors and actuators [8], energy harvesting [9] or biomedical applications [10], due to their large deformation, flexibility and tailored electrical conductivity [3,11,12].

Applications of conductive polymer composites in sensor applications include strain, damage and temperature variation detection, among others [3]. In particular, elastomer composites with conductive fillers show strong piezoresistive properties, which are being used for the development of large deformation sensors [13]. The wide range of applications of strain sensing include smart textiles, structural and health monitoring, and movement sensors, among others [14]. Several of these sensor applications imply that materials are subjected to varying environmental conditions. In a similar way, recent application areas of these materials such as dielectric elastomers actuators (DEA) [15] and energy harvesters [15,16] imply the outdoors implementation of the materials.

There is a wide variety of thermoplastics used in industrial applications, TPEs being increasingly used in a larger number of areas [17]. SBS is a TPE sensitive to degradation [17], the elastomeric polybutadiene (PB) phase being more susceptible to degradation than the polystyrene phase (PS) [18]. Thus, the copolymer styrene-ethylene/butadiene-styrene (SEBS) has been developed to overcome the degradation problems of SBS. SEBS is obtained from the hydrogenation of SBS, a process that allows removing the unsaturation typical of the butadiene components (carbon-carbon double bonds are saturated with hydrogen) with a positive effect on environmental, thermal and UV radiation resistance, while maintaining thermoplastic behavior [17]. With respect to the potential use for biomedical applications, SEBS and SBS C540 show no cytotoxic behavior, contrary to the SBS composite materials with CNT that showed cytotoxic behavior [19].

As previously mentioned, a large number of promising applications of TPE take place in an outdoor environment and are subjected to temperature and humidity variations, UV radiation, etc. In particular, ageing of SBS and SEBS, due to the presence of the PB blocks, can lead to reduction of their mechanical, thermal, electrical and electromechanical properties [20].

Oxygen and UV radiation are the most important factors contributing to the degradation of polymer materials by chemical modification at the molecular level, due to their high sensitivity to oxidation by photo-oxidation mechanisms [21]. These factors promote the formation of oxidized groups involving chain scissions and the formation of new covalent bonds between chains, resulting in the deterioration of material properties [21]. It has been shown that SEBS shows higher UV and ozone resistance than SBS [17,18] but there are no systematic studies on the effect of UV ageing on the mechanical and electrical properties of these important materials, including their composites with CNT. Therefore, several triblock copolymer of SBS, with different block structures, butadiene/styrene ratio and CNT filler contents have been investigated, together with SEBS, as regards the effect of UV ageing.

Experimental

Commercial tri-block copolymers of SBS with references Calprene C401, C411 and C500, and SEBS 6120 (main properties summarized in Table 1) were kindly supplied by Dynasol Gestión, SA (Spain). The copolymers show two different butadiene/styrene (B/S) ratios and two different structures (radial and linear). For the development of the polymer composites, multi-walled carbon nanotubes (MWCNT) from Nanocyl with reference NC7000 were used. The CNT show purity of 90%, outer mean diameter of 9.5 nm and length of 1.5μ m.

Sample preparation

Polymer films were prepared using toluene as solvent in a ratio of 6 mL of toluene to 1 g of SBS or SEBS. The copolymers and toluene were placed in an Erlenmeyer flask and stirred until complete dissolution was achieved. Thin and highly flexible films were obtained by spreading the solution on a clean glass substrate. The evaporation of toluene was performed at room temperature for 12 h .

For the preparation of the nanocomposites, the relevant weight of CNT was placed in an Erlenmeyer flask with toluene and kept in an ultrasound bath (Bandelin, Model Sonorex Super RK106) for 6 h to promote good MWCNT dispersion. After this stage, the copolymer was added to the toluene/CNT solution and stirred until complete dissolution. Then, the same experimental procedure as for the pure polymers was applied. The thickness of the obtained films was 100μ m for C401, 160μ m for C411, 255μ m for C500, 230μ m for SEBS and 160μ m and 230μ m for the composites with 0.25 and 1wt% CNT content. The error in the determination of the thickness is $\sim$ 5μ m.

Ageing procedure

Accelerated ageing experiments were carried out in a Xenotest 150 S chamber from Heraeus (Original Hanau) equipped with a filtered Xenon lamp with an intensity of 60Wm^{-2} according to standard procedures (ISO-4892 Plastics-Methods of Exposure to

Laboratory Light SourcesPart2: Xenon-arc Sources, International Organization for Standardization, and to ASTM D1435-Standard Practice for Outdoor Weathering of Plastics). The Xenon lamp light was filtered between 600 to 300 nm with an UV window combined with six IR filter glasses.

Samples with dimensions 100 mm × 25 mm were exposed to several degradation times. During each ageing cycle of 2 h the samples were exposed to 18 ± 0.5 min of

Table 1
Main characteristics of the SBS and SEBS samples.

Samples	SBS C401	SBS C411	SBS C500	SEBS CH-6120
Butadiene/Styrene ratio	80/20	70/30	70/30	68/32
Block structure	Radial	Radial	Linear	Linear
CNT (wt%)	0	0	0	0
	1			

rain and the remaining time, 102 ± 0.5 min, was considered a dry period. The evolution of the temperature and relative humidity in each degradation cycle is shown in Table 2. Accelerated degradation of samples was measured in intervals of 8 h(4 cycles of 2 h), with 408 min of dry period and 72 min of rain period, up to a maximum degradation time of 88 h .

The accelerated ageing time can be correlated with the outdoor conditions. It has been shown [22] that one year of exposure time to outdoor conditions in the city of Lisbon represents $\sim 207 \mathrm{MJ.\,m^{-2}}$. In [22], 1260 h of accelerated ageing with an acceleration factor of $\kappa \sim 0.85$ is similar to one year in outdoor conditions in Lisbon [22]. Under the conditions used in the present work, 80 h in the Xenotest set-up represent an energy of $\sim 17.28 \mathrm{MJ.\,m^{-2}}$, which results in ~ 36 days of exposure to outdoor conditions in Lisbon, using a similar accelerated factor as in [22]. It has been also reported that accelerated photooxidation ranges from 2.5 to 10 times when compared to outdoor exposure [18].

Sample characterization

Fourier Transformed Infrared spectroscopy (FTIR) was performed at room temperature with a Jasco FT/IR-4100 spectrometer. FTIR spectra were collected in attenuated total reflectance mode (ATR) from 4000 to 600 $\mathrm{cm^{-1}}$ after 32 scans with a resolution of 4 $\mathrm{cm^{-1}}$.

UV tests were performed in a double beam UV-2501PC UV/VIS spectrophotometer from 200 to 500 nm using a solid film support.

Atomic force microscopy (AFM) measurements were performed using the tapping mode of a MultiMode set-up connected to a NanoScopeIII, both from Veeco, USA, with non-contacting silicon cantilevers (ca. $47 - 76\mathrm{kHz}$, k: $1.2 - 6.4\mathrm{Nm^{-1}}$) from App-Nano, USA. All images (2μ m wide) were fitted to a plane using the1st degree flatten procedure included in the NanoScope software version 4.43rd8. The surface roughness was

calculated as Sq (root mean square from average flat surface) and Sa (average absolute distance from average flat surface).

Mechanical measurements were performed at room temperature on a universal testing machine Shimadzu model AG-IS with a load cell of 50 N in tensile mode. Rectangular samples were used with dimensions of 60 mm × 20 mm at a test velocity of 2 mm/min. The initial modulus was determined from the obtained results up to 3% strain.

Table 2
Temperature and relative humidity variations during each of the 120 min ageing cycles.

Time (min)	Temperature (°C)	Humidity (%)
0	21.3	75.0
15	27.5	79.2
30	31.3	71.7
45	31.9	70.6
60	32.3	69.9
75	32.7	69.2
90	32.8	69.0
105	33.1	68.4
120	33.2	68.0

Electrical resistance of the composites was calculated from the slope of I-V curves measured with an automated Keithley 487 picoammeter/voltage source. Previously, 5 mm diameter Au contacts were deposited on both sides of the composites with a Polaron SC502 sputter coater. Volume resistivity was determined with an applied voltage ranging between -10 and +10 V and measuring the current. The electrical resistivity of the composites (ρ) was calculated by:

$$\rho = \frac{RA}{d} \tag{1}$$

where R is the resistance of the composite, A the area of the electrodes and d is the sample thickness. The electrical conductivity is the inverse of electrical resistivity.

Water contact angle (WCA) of the samples was measured by the static sessile drop method using a Data Physics OCA20 instrument with ultrapure water. WCA was measured by depositing water drops (3μ L) onto a sample surface and determined using the SCA20 software. Each sample was measured at six different locations on each sample and the mean contact angle and standard deviation was calculated.

Cytotoxicity tests

Membrane sterilization: For the in vitro assays, circular samples of 13 mm diameter were cut from films after different degradation times and sterilized by multiple immersions into 70% ethanol for 30 min each, followed by washing 5 times in a phosphate buffer saline (PBS) solution for 5 min to remove any residual solvent. Subsequently, the samples were exposed to ultraviolet (UV) light for 1 h .

Cell culture: C2C12 mouse myoblast cells were grown in 75 cm^2 cell culture flasks using Dulbecco's Modified Eagles' Medium (DMEM, Gibco) containing 4.5 g. L^{-1} glucose supplemented with 10% Fetal Bovine Serum (FBS, Biochrom) and 1% Penicillin/Streptomycin (P/S, Biochrom). The cells were incubated under standard culture conditions at 37°C in a 95% humidified air containing 5%CO_2 atmosphere. The culture medium was changed every two days and when the cells reached the confluence (60 – 70%), they were trypsinized with 0.05% trypsin-EDTA.

Cytotoxicity assay: The extraction media were prepared by immersing the samples (13 mm of diameter) in 24 -well tissue culture polystyrene plates with DMEM, containing 4.5 g. L^{-1} glucose supplemented with 10% FBS and 1%P/S, under standard culture conditions (37°C in a 95% humidified air containing 5%CO_2) and incubated for 24 h . At the same time, C2C12 cells were seeded in the 96-well tissue culture polystyrene plates at a density of 2×10^4 cells mL^{-1} and incubated for 24 h to allow cell attachment on the plates. After 24 h , the culture medium was removed and the as-prepared extraction media were added to the cells (100μ L). Then, the cells were incubated for 24 h and 72 h and the number of viable cells was quantified by MTT (3 [4,5-dimethylthiazol-2-yl]-2,5 diphenyltetrazolium bromide) colorimetric assay after each incubation time. The cells received MTT solution (5mg. mL^{-1} of MTT dissolved in DMEM in proportion of 1: 10 respectively) and were

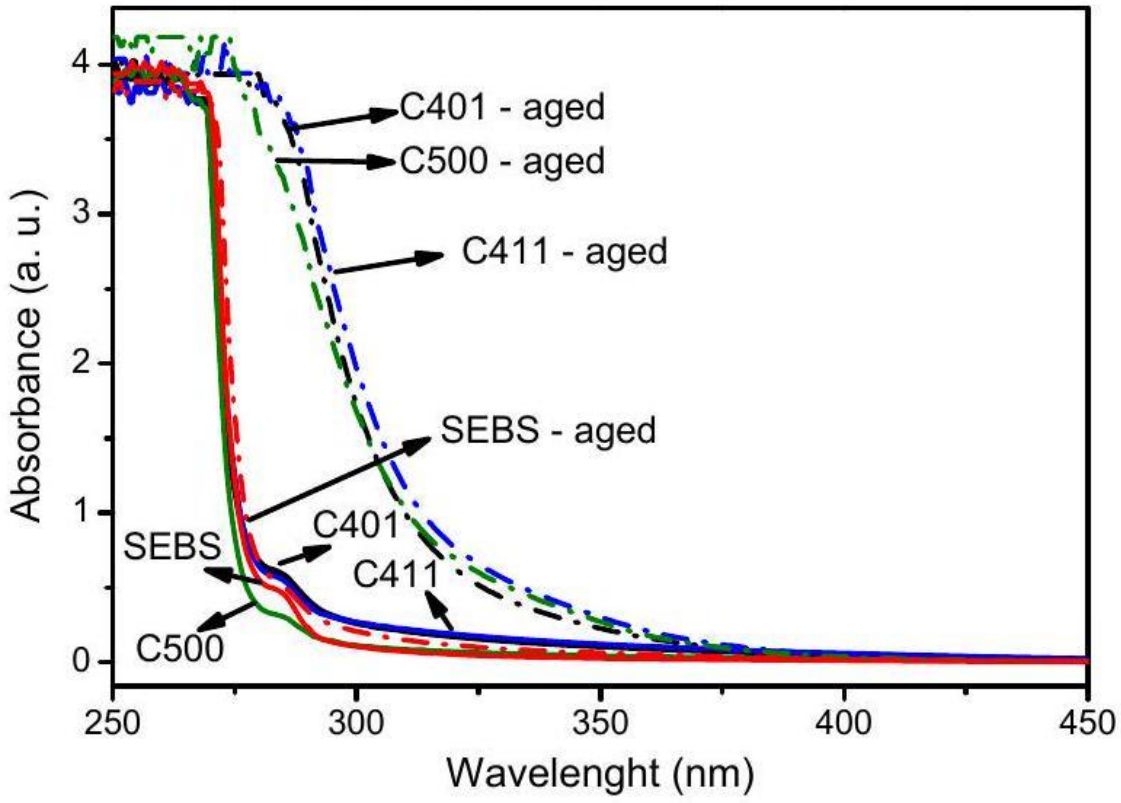

Fig. 1. UV spectra of the C401, C411 and C500 SBS samples and the SEBS sample before and after 80 h aging in a Xenontest set up. Composite samples with CNT show no UV transmittance.

incubated in the dark at 37°C for 3 h . After that, the MTT solution was removed and the precipitated formazan was dissolved in 100μ L dimethylsulfoxide (DMSO). Quantification was performed by measuring the absorbance at 570 nm using a microplate reader.

Results and discussion

Evaluation of chemical modifications

Yellowing of polymer materials during processing and lifetime is an important indication of degradation processes that can decrease material performance. Color modifications during weathering are due to the formation of photoproducts such as carbon-carbon double bonds [23]. Fig. 1 shows the UV spectra of the pristine copolymer samples before and after 80 h exposure to a Xenon lamp. The slight absorbance variations observed for SEBS indicates that this material is less susceptible to weathering, being stable during the 80 h under test. However, significant differences are observed in the SBS samples, independently of their block structure or copolymer styrene/butadiene relative content. Composites samples (0.25 and 1wt% CNT) do not show any transmittance in the UV measurements.

The observed absorbance variation can attributed to the formation of α and β-unsaturated ketones that occur after UV ageing [24].

FTIR-ATR is an important tool to understand polymers ageing, allowing the identification of structural changes at a molecular level. Fig. 2 shows the FTIR-ATR spectra of some representative samples indicated in Table 1. Fig. 2A corresponds to the C401 sample and is representative of the samples undergoing degradation. Fig. 2B, on the other hand, corresponds to SEBS and is representative of the samples showing UV degradation stability. The behavior for the rest of the samples is similar to either one or the other category, as indicated later.

For all samples, differences are noticed mainly in the hydroxyl ($3000 - 3400\ cm^{-1}$), carbonyl ($1600 - 1800\ cm^{-1}$) and butadienic phase (911 and 965 cm^{-1} for the hydrogen atoms correspond to the trans $C = C$ unsaturation (vinyl) in polybutadiene and the 1,2 butadiene terminal vinyl C-H band, respectively) [25]. The variation observed in the samples undergoing degradation were always at the same wavenumbers, indicating that the same photoproducts were formed and, therefore, that the same degradation mechanism occurred in all SBS samples. On the other hand, SBS composites with CNT and SEBS showed no degradation.

From the FTIR-ATR spectra of Fig. 2, the absorbance of some specific relevant bands as a function of degradation time (Fig. 3) was obtained. A decrease in the absorbance of the characteristic butadiene bands can be observed (Fig. 3 A and B, respectively for 911 and 966 cm^{-1}) due to unsaturated butadiene chains [23] and the emergence of carbonyl (1715 cm^{-1}) and hydroxyl (3400 cm^{-1}) bands, Fig. 3C and D respectively, due to the formation of esters, lactones and alcohols [23,25], respectively. The absorbance variation over accelerated ageing time of the characteristics bands occurs for the SBS matrices for

times above 60 h . No significant changes are detected for the SEBS copolymer (Fig. 3).

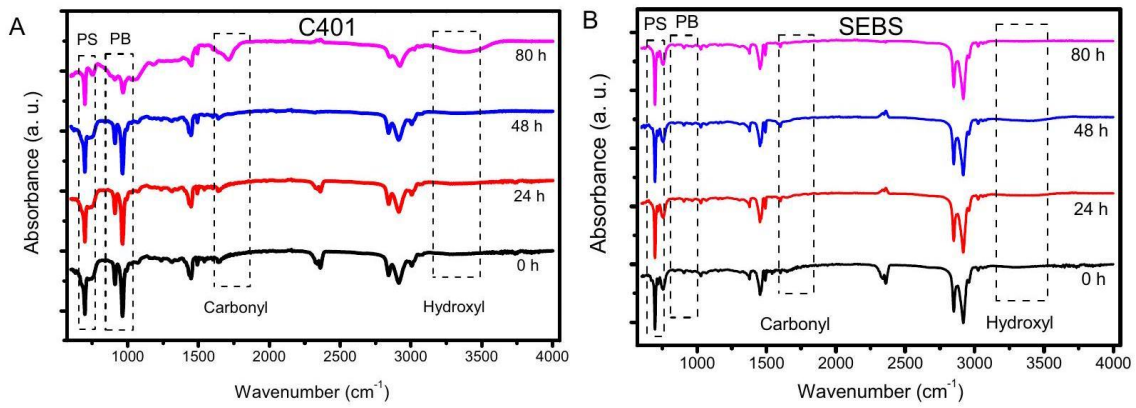

Fig. 2. Representative FTIR-ATR spectra obtained for a C401 sample (A) and a SEBS sample (B) after 0, 24, 48 and 80 h UV accelerated ageing time in the Xenontest set-up.

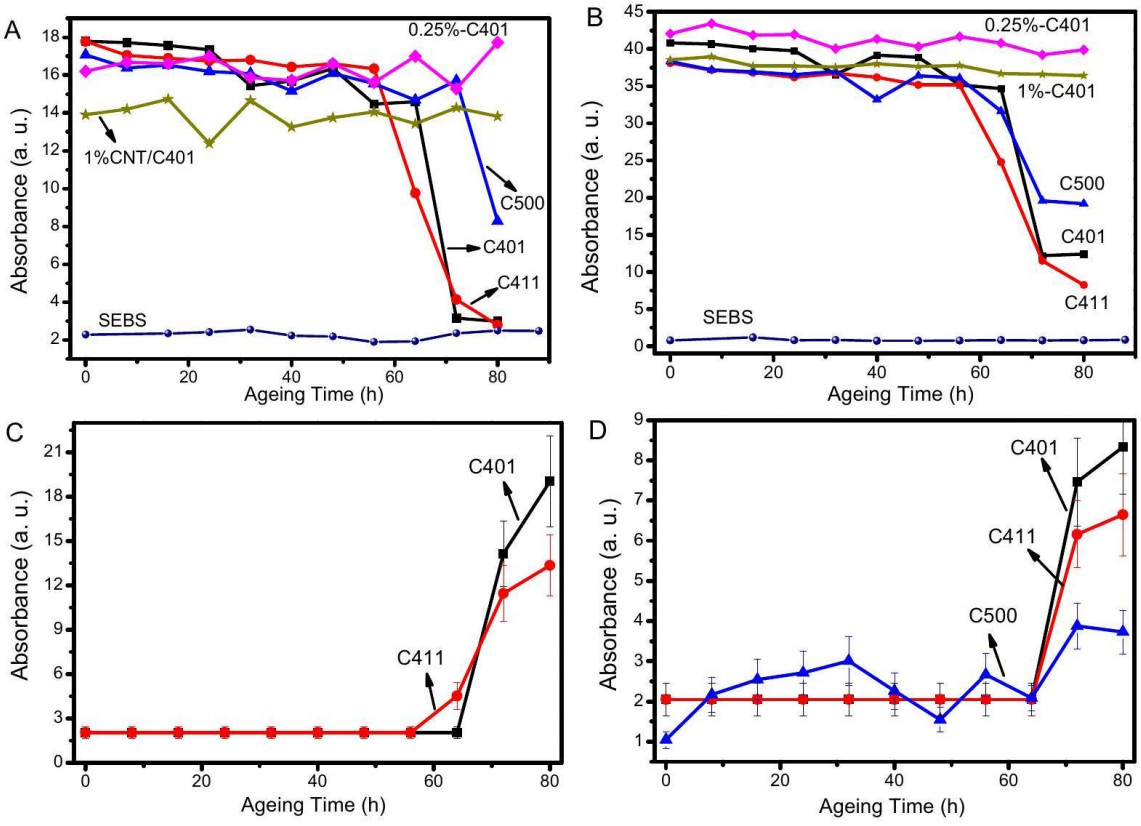

Fig. 3. FITR-ATR absorbance at (A) 911, (B) 966, (C) 1720 and (D) 3400 cm^{-1} as a function of UV accelerated ageing time.

Fig. 3A shows the evolution of the absorbance of the butadiene bands over UV ageing time. The absorption bands of butadiene at 911 and 966 cm^{-1} decrease due to radical cleavage of the PB chain [26,27]. The decrease of 1,4 PB(966 cm^{-1}) content is more pronounced

than that of 1,2 PB(911 cm^{-1}), which is in agreement with the results presented in [22,28]. For both butadiene characteristics bands, C401 and C411 samples show similar behavior, with a slight decrease up to 60 h of ageing time and a strong decrease after this time. The C500 sample shows identical behavior for the wavenumber of 966 cm^{-1} but, on the other hand, the strong decrease of the 911 cm^{-1} absorption band occurs just after 80 h ageing time. Thus, it is possible to correlate the B/S ratio and block structure with the degradation process, the samples with radial block structure and larger butadiene content showing higher degradation of the butadiene chains. Further, it is observed that the degradation is abrupt between 60 and 70 h of ageing, and then stabilizes after this initial degradation step for both butadiene chains.

The introduction of CNT to the polymer seems to practically inhibit the degradation, as the decrease of both butadienic bands is much slower and only a small decrease of the absorption bands is detected. This suggest that CNT works as a photostabilizer in the composites. Similar behavior has been previously reported in other polymer matrices [29-31]. The photostabilization of composites due to CNT has been ascribed to the effect of the electron ring of the CNT network, which can disperse and filter the UV energy, as well as the strong interaction between free radicals (generated during irradiation) and the CNT [29,30]. The butadiene characteristic bands (911 and 966 cm^{-1}) are less pronounced in the SEBS matrix, as observed in Fig. 2B. The SEBS shows higher photodegradation resistance, showing no degradation up to the 88 h of exposure time, as reported in [32,33].

The degradation of SBS is, as previously mentioned, attributed to the PB chains, the PS chains being less susceptible to photodegradation and requiring much longer time to suffer degradation when exposed to radiation [20,34]. In fact, the styrene characteristic band at 699 cm^{-1} does not suffer any change during the entire ageing exposure time.

During sample degradation, the carbonyl and hydroxyl group formations show two stages (Fig. 3C and D): first a slow formation of both carbonyl (1715) and hydroxyl (3400) groups occurs, which is followed by an accelerated ageing with faster formation of the same groups. The strong absorbance increase of the infrared bands associated with both groups occurs around 60 h , correlated to the previously mentioned decrease of the butadiene bands in the pure polymers. By comparing the different SBS matrices, it can be observed that the increase is higher for the C401 sample than for C411; the C500 matrix showing the lowest increase for the hydroxyl group and no absorbance indicating the presence of carbonyl groups up to the 80 h of accelerated ageing time. These results confirm that radial block structure and larger butadiene content lead to stronger weathering degradation. Further, the inclusion of CNT leads to higher UV stability and, for both composites with 0.25 and 1wt% CNT content in the C401 matrix, no absorption bands indicating the presence of carbonyl or hydroxyl bands are observed. In the same way, SEBS also shows UV stability and no absorbance corresponding to carbonyl or hydroxyl bands are detected.

Effect of UV accelerated ageing on surface morphology

The effect of UV accelerated ageing on surface morphology of the copolymers was analyzed by AFM before and after UV exposure, as shown in Fig. 4 for the C401 sample.

Fig. 4 b shows an increase of the surface roughness of the C401 sample after an UV exposure time of 80 h compared to the non-aged sample (Fig. 4a). The UV radiation creates microcracks on the surface of the samples [35], which will influence the mechanical properties, with a decrease of the maximum strain on the aged samples when compared to the non-aged ones (see Section 3.3).

Mechanical properties

Characteristic stress-strain curves of the different materials before and after 80 h of accelerated ageing are presented in Fig. 4. Table 3 shows the variations in the maximum strain.

It has been previously demonstrated that more degradation occurs in C401 and C411 samples, followed by C500. Moreover, the introduction of CNT to the polymer matrix prevents polymer degradation and the SEBS polymer does

Table 3
Strain at break before (0 h) and after 80 h UV accelerated ageing time for the C401, C411, C500 and SEBS samples as well as for the C401 composites with 0.25 and 1wt% CNT.

Samples	ε_{break} (%)	
	0 h	80 h
C401	1081 ± 85	8 ± 2
C411	933 ± 88	216 ± 15
C500	924 ± 91	760 ± 85
SEBS	1559 ± 118	1054 ± 102
0.25%-C401	1080 ± 102	411 ± 33
1%-C401	1140 ± 95	709 ± 65

not seem to undergo degradation. This behavior is reflected in the mechanical properties, where the maximum deformation obtained for the C401 and C411 samples suffers a strong decrease after 80 h of UV accelerated ageing, as shown in Fig. 5 and Table 3.

As butadiene plays the most relevant role in the degradation of the samples, the SBS samples with larger amount of butadiene show a stronger decrease in the maximum deformation. Thus, after 80 h of accelerated ageing, the C401 SBS sample loses the rubber-like behavior characteristic of the non-aged samples. On the other hand, the mechanical properties of the SEBS and C500 samples remain almost as in the pure samples. Copolymer block structure, radial or linear, also influences the mechanical properties. Both C411 and C500 copolymers show 70/30 B/S ratio with radial and linear structure and a maximum deformation of 216% and 760%, respectively. Therefore, for similar butadiene content, the linear block structure shows larger deformation than the radial structure. It is noteworthy that, for pure C401 and C500 samples, the maximum deformation before degradation is similar for both copolymers, 924% and 933%, respectively (Table 3). The linear copolymer shows higher resistance to accelerated ageing

than the radial copolymer, as can be observed

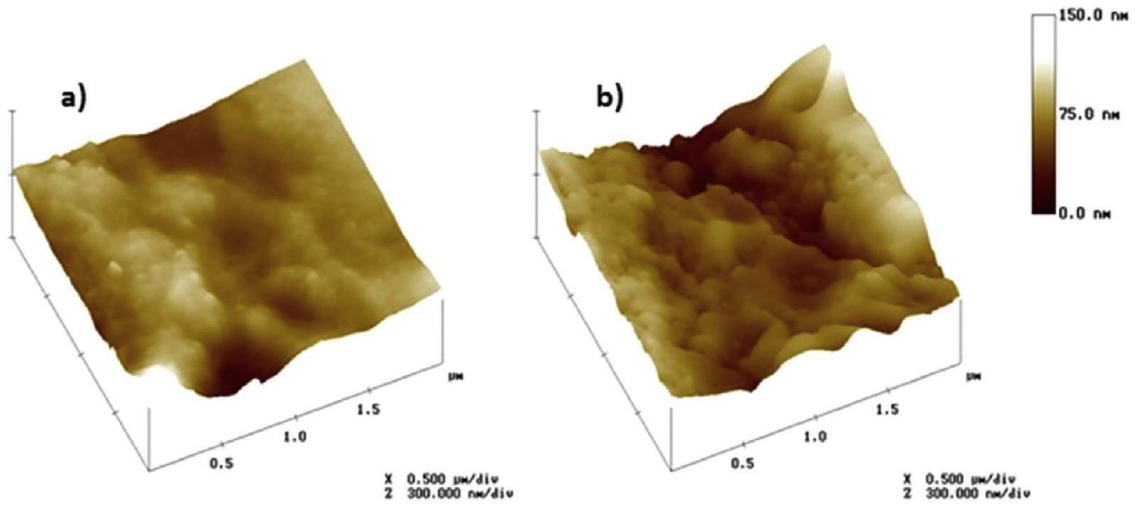

Fig. 4. AFM images showing the surface roughness of the C401 sample before (a) and after 80 h (b) accelerated ageing time.

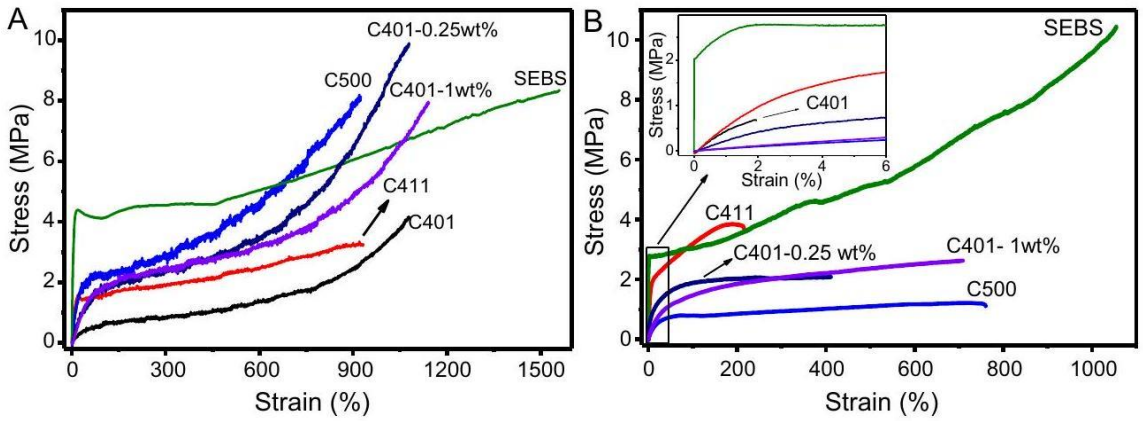

Fig. 5. Stress-strain curves for the C401, C411, C500, SEBS and C401 composite with 0.25 and 1wt% CNT before (A) and after 80 h (B) accelerated ageing time (B). The inset in figure B represents the initial 6% of strain in order to observe the C401 stress-strain curve.
by the mechanical and FTIR-ATR (Fig. 3) results. The roughness variations observed in the AFM image can explain this abrupt decrease in the maximum deformation of C401 copolymer, together with the variation at the molecular level. CNT inclusion in the SBS matrix prevents ageing and increases the mechanical properties of aged composites. In this way, aged C401 without CNT has maximum deformation of 8%, increasing to 411% and 709% with CNT content of 0.25 and 1wt%, respectively. SEBS after 80 h of UV exposure still shows maximum deformations above 1000%.

Electrical conductivity

The electrical conductivity of the composites with 0.25 and 1wt% CNT content in the C401 matrix is shown in Fig. 6. The electrical conductivity increases with increasing CNT

content [6] and shows a slight decrease with increasing UV accelerated ageing time. The samples without CNT loading show electrical conductivities of the order of 3×10^{-11}(S/ m), and the composite samples with different CNT content do not suffer large variation with ageing time (Fig. 6). In this sense, polymer degradation

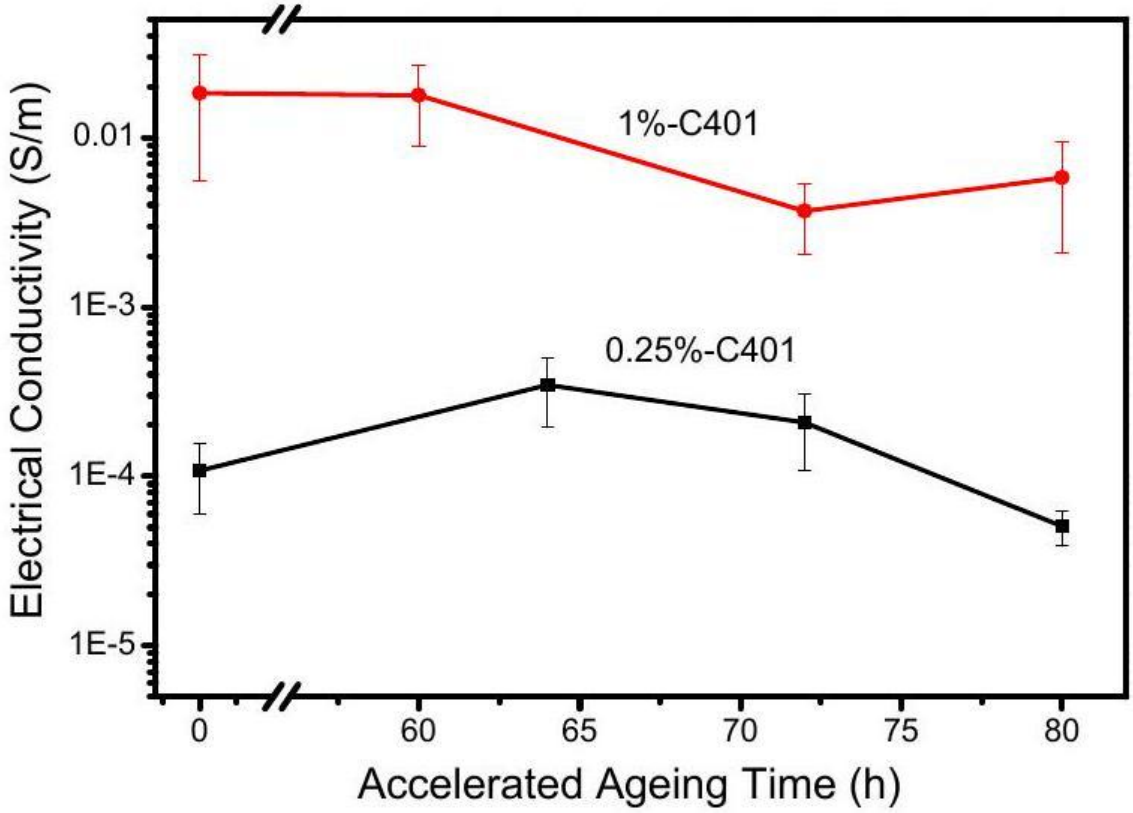

Fig. 6. Electrical conductivity of the C401 SBS composites with 0.25 and 1 wt % CNT content as a function of accelerated aging time. does not significantly affect the electrical properties of the elastomers.

Surface contact angle

For tissue and biomedical engineering applications, the surface wettability of the materials is an important parameter as it plays a relevant role in cell attachment. The WCA of the different samples before and after accelerated ageing up to 80 h is presented in Fig. 7.

Solvent casted films before ageing show WCA values around 100° both for SBS and SEBS, also being independent of the CNT content and block structure. Films subjected to 80 h accelerated ageing by UV radiation show a significant decrease of WCA for all samples, leading to more hydrophilic behavior. The WCA decrease for the C401 and C411 films is larger, reaching values around 50°. The samples with radial block structure (C401 and C411) exhibit a larger decrease than those with a linear block structure (C500 and SEBS) with WCA values around 80°. The introduction of CNT fillers in the C401 films leads to WCA values of the samples after 80 h UV accelerated ageing of ~ 60° for 0.25% C401 and ~ 80° for 1%-C401. Finally, SEBS samples demonstrated a significant decrease of the WCA

after 72 h ageing.

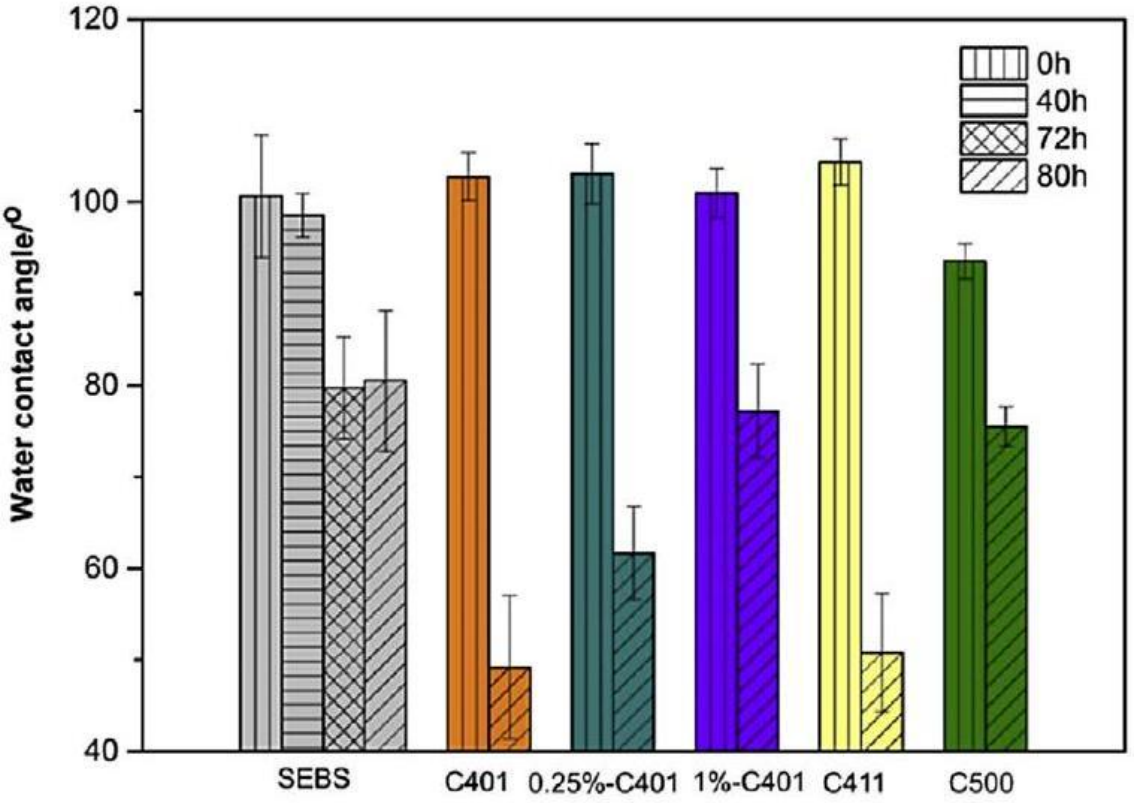

Fig. 7. Water contact angle of the different SBS and SEBS samples before and after different accelerated ageing times.

It is thus shown that the time necessary to cause modification of the wettability of the surface is between 40 and 72 h , and that the general trend is a decrease of the WCA, mainly attributed to sample surface variations (Fig. 4), which can influence positively cell response [36].

Cytotoxicity

The cytotoxicity of the different SBS and SEBS samples before and after different UV ageing times was evaluated by the MTT assay method against C2C12 myoblast cell line. The results are presented in Fig. 8.

It has been shown that SEBS samples are not cytotoxic to C2C12 cells [19]. Fig. 8 shows that this fact is effectively verified for SEBS before exposure, as cell viability at 24 h exhibit values close to 100%, and after 72 h there is just a slight decrease in cell viability to values around 85%. According to ISO standard 10993-5, samples are considered cytotoxic when the cell viability reduction is larger than 30%. Increasing SEBS ageing time does not lead to cytotoxic samples, the cell viability values after 72 h ranging between 86 and 92%. Similar results were obtained for pristine SBS films (C401-, C411- and C500 SBS), showing cell viability before UV ageing, as has been previously shown for C540 SBS [19]. However, when these samples undergo UV ageing, the cell viability values after 24 h of the samples with radial block structure, C401 and C411, fall to ~ 5% and ~ 40%, respectively. This

represents cytotoxic behavior after only 24 h degradation time, indicating the presence of the polymer degradation products. For the C500 samples, the cell viability values range around ~ 80% after 24 h (no cytotoxicity) becoming cytotoxic with increasing degradation time up to 72 h (~ 5% cell viability). Hence, these C401, C411 and C500 films are cytotoxic to C2C12 cells. Relative to the introduction of CNT fillers, it was previously observed that they strongly reduce the degradation of the polymer matrix. This fact, on the other hand, does not prevent the samples becoming cytotoxic after

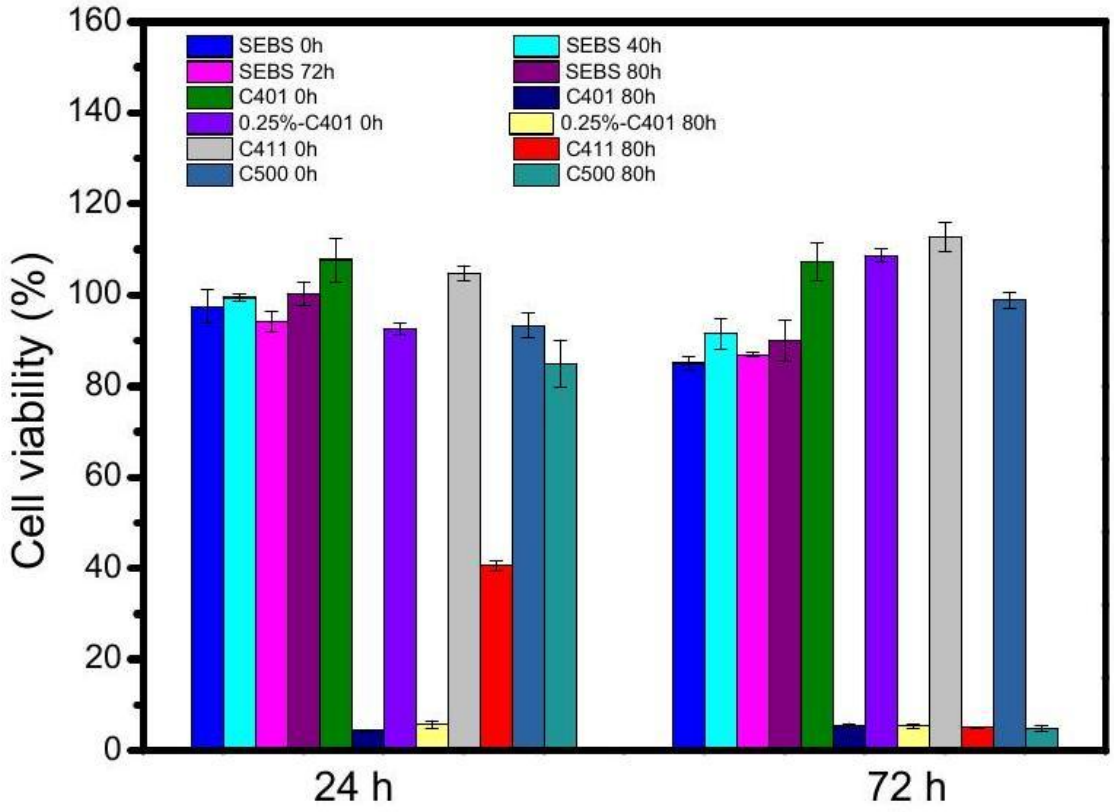

Fig. 8. MTT cytotoxicity assays of C2C12 cells in contact with as-prepared extraction media exposed to C401, C401 composites with 0.25 wt% CNT content (0.25%-C401), C411 and C500 samples before (0 h) and after 80 h accelerated ageing time and to SEBS samples after 0 h, 40 h, 72 h and 80 h ageing time.

UV exposure, i.e. there is a reduction of the degradation product but still at a cytotoxic level.

Conclusions

Thermoplastic elastomers are interesting materials due to their excellent mechanical properties such as large deformation and fast recovery after applied stress, and can be used in a wide range of indoor and outdoor applications. Accelerated ageing studies show that photodegradation affects essentially the butadiene phase of the copolymers, with characteristics absorbance bands at 911 and 966 cm^{-1} that decrease with increasing ageing time. The degradation is stronger for copolymers with larger amount of butadiene and

radial block structure. Mechanical properties corroborate the FTIR-ATR analyses and the copolymer with larger amount of butadiene shows lower maximum deformation. Almost no chemical changes were detected for polymer composites with CNT and SEBS. The hydrophobicity of the samples decrease with increasing ageing time, mainly due to polymer surface modifications. UV ageing also influences the cytotoxicity of the SBS samples but not the SEBS ones: after UV accelerated ageing, only the SEBS samples remain non cytotoxic. In this way, SEBS is the most suitable copolymer for outdoor and biomedical applications due to UV ageing resistance when compared to the SBS matrices.

Acknowledgements

This work is funded by FEDER funds through the "Programa Operacional Fatores de Competitividade COMPETE" and by national funds arranged by FCTFundação para a Ciência e a Tecnologia, project references PTDC/CTM-NAN/112574/2009, PEST-C/FIS/UI607/2014 and PEST-C/QUI/UIO686/2013. The authors also thank funding from Matepro -Optimizing Materials and Processes, ref. NORTE-07-0124-FEDER-000037, co-funded by the "Programa Operacional Regional do Norte" (ON. 2 - O Novo Norte), under the "Quadro de Referência Estratégico Nacional" (QREN), through the "Fundo Europeu de Desenvolvimento Regional" (FEDER) and the n-STeP Project, reference NORTE-07-0124-FEDER-000039, supported by the Programa Operacional Regional do Norte (ON.2). PC thank the FCT for the SFRH/BD/64276/2009 grant. Thanks to Dynasol (Spain) by supply several thermoplastic elastomers.

References

[1] E. Yousif, R. Haddad, Photodegradation and photostabilization of polymers, especially polystyrene: review, SpringerPlus 2 (2013) 398.
[2] A.D. Drozdov, J. Christiansen, Thermo-viscoplasticity of carbon black-reinforced thermoplastic elastomers, Int. J. Solids Struct. 46 (2009) 2298-2308.
[3] M. Ji, H. Deng, D. Yan, X. Li, L. Duan, Q. Fu, Selective localization of multi-walled carbon nanotubes in thermoplastic elastomer blends: an effective method for tunable resistivity-strain sensing behavior, Compos. Sci. Technol. 92 (2014) 16-26.
[4] J.H. Wu, C.H. Li, Y.T. Wu, M.T. Leu, Y. Tsai, Thermal resistance and dynamic damping properties of poly (styrene-butadiene-styrene)/ thermoplastic polyurethane composites elastomer material, Compos. Sci. Technol. 70 (2010) 1258-1264.
[5] H. Lorenz, J. Fritzsche, A. Das, K.W. Stöckelhuber, R. Jurk, G. Heinrich, et al., Advanced elastomer nano-composites based on CNT-hybrid filler systems, Compos. Sci. Technol. 69 (2009) 2135-2143.
[6] P. Costa, J. Silva, V. Sencadas, R. Simoes, J.C. Viana, S. LancerosMéndez, Mechanical, electrical and electro-mechanical properties of thermoplastic elastomer styrene-butadiene-styrene/multiwall carbon nanotubes composites, J. Mater. Sci. 48 (2012) 1172-1179.
[7] Z.M. Dang, K. Shehzad, J.W. Zha, A. Mujahid, T. Hussain, J. Nie, et al., Complementary percolation characteristics of carbon fillers based electrically percolative thermoplastic elastomer composites, Compos. Sci. Technol. 72 (2011) 28-35.
[8] P. Brochu, Q. Pei, Advances in dielectric elastomers for actuators and artificial muscles, Macromol. Rapid Commun. 31 (2010) 10-36.
[9] K.K. Sadasivuni, D. Ponnamma, S. Thomas, Y. Grohens, Evolution from graphite to graphene elastomer composites, Prog. Polym. Sci. 39 (2014) 749-780.

[10] D.J. Martin, A.F. Osman, Y. Andriani, G.A. Edwards, 11-Thermoplastic polyurethane (TPU)-based polymer nanocomposites, in: F. Gao (Ed.), Advances in Polymer Nanocomposites, Woodhead Publishing, 2012, pp. 321-350.
[11] W. Zhi Feng, W. Pei, Y. Xiong Ying, J. Bo, Processing and modeling of multi-walled carbon nanotube/styrene- butadiene-styrene (SBS) composites for force sensing, in: leee-nano 2009 9th IEEE Conference on Nanotechnology 2009, 2009, pp. 756-757.
[12] P.J. Cottinet, D. Guyomar, J. Galineau, G. Sebald, Electro-thermoelastomers for artificial muscles, Sensor Actuat a-Phys. 180 (2012) 105-112.
[13] W. Yi, Y. Wang, G. Wang, X. Tao, Investigation of carbon black/silicone elastomer/dimethylsilicone oil composites for flexible strain sensors, Polym. Test. 31 (2012) 677-684.
[14] H. Deng, L. Lin, M. Ji, S. Zhang, M. Yang, Q. Fu, Progress on the morphological control of conductive network in conductive polymer composites and the use as electroactive multifunctional materials, Prog. Polym. Sci. 39 (2014) 627-655.
[15] D.L. Henann, S.A. Chester, K. Bertoldi, Modeling of dielectric elastomers: design of actuators and energy harvesting devices, J. Mech. Phys. Solids 61 (2013) 2047-2066.
[16] I.J. Kim, K. Min, H. Park, S.M. Hong, W.N. Kim, S.H. Kang, et al., Mechanical, dielectric, and electromechanical properties of silicone dielectric elastomer actuators, J. Appl. Polym. Sci. 131 (2014) (n/a-n/a).
[17] D. Juárez, S. Ferrand, O. Fenollar, V. Fombuena, R. Balart, Improvement of thermal inertia of styrene-ethylene/butylene-styrene (SEBS) polymers by addition of microencapsulated phase change materials (PCMs), Eur. Polym. J. 47 (2011) 153-161.
[18] C.C. White, K.T. Tan, D.L. Hunston, T. Nguyen, D.J. Benatti, D. Stanley, et al., Laboratory accelerated and natural weathering of styr-ene-ethylene-butylene-styrene (SEBS) block copolymer, Polym. Degrad. Stab. 96 (2011) 1104-1110.
[19] Ribeiro S, Costa P, Ribeiro C, Sencadas V, Botelho G, LancerosMéndez S. Electrospun styrene-butadiene-styrene elastomer copolymers for tissue engineering applications: effects of butadiene/ styrene ratio, block structure, hydrogenation and carbon nanotube loading. 2014.
[20] R.P. Singh, S.M. Desai, S.S. Solanky, P.N. Thanki, Photodegradation and stabilization of styrene-butadiene-styrene rubber, J. Appl. Polym. Sci. 75 (2000) 1103-1114.
[21] G. Mertz, F. Hassouna, P. Leclère, A. Dahoun, V. Toniazzo, D. Ruch, Correlation between (nano)-mechanical and chemical changes occurring during photo-oxidation of filled vulcanised styrene butadiene rubber (SBR), Polym. Degrad. Stab. 97 (2012) 2195-2201.
[22] R.M. Santos, G.L. Botelho, A.V. Machado, Artificial and natural weathering of ABS, J. Appl. Polym. Sci. 116 (2010) 2005-2014.
[23] B. Singh, N. Sharma, Mechanistic implications of plastic degradation, Polym. Degrad. Stab. 93 (2008) 561-584.
[24] X. Jouan, J.L. Gardette, Photo-oxidation of ABS: part 2-Origin of the photodiscoloration on irradiation at long wavelengths, Polym. Degrad. Stab. 36 (1992) 91-96.
[25] R.M. Santos, G.L. Botelho, C. Cramez, A.V. Machado, Outdoor and accelerated weathering of acrylonitrile-butadiene-styrene: a correlation study, Polym. Degrad. Stab. 98 (2013) 2111-2115.
[26] V. Mouillet, F. Farcas, S. Besson, Ageing by UV radiation of an elastomer modified bitumen, Fuel 87 (2008) 2408-2419.
[27] M.D. Romero-Sánchez, M.J. Walzak, R. Torregrosa-Maciá, J.M. Martín-Martínez, Surface modifications and adhesion of SBS rubber containing calcium carbonate filler by treatment with UV radiation, Int. J. Adhesion Adhesives 27 (2007) 434-445.
[28] J.G. Bokria, S. Schlick, Spatial effects in the photodegradation of poly(acrylonitrile-

butadiene-styrene): a study by ATR-FTIR, Polymer 43 (2002) 3239-3246.
[29] E.J. Petersen, T. Lam, J.M. Gorham, K.C. Scott, C.J. Long, D. Stanley, et al., Methods to assess the impact of UV irradiation on the surface chemistry and structure of multiwall carbon nanotube epoxy nanocomposites, Carbon 69 (2014) 194-205.
[30] E. Najafi, K. Shin, Radiation resistant polymer-carbon nanotube nanocomposite thin films, Colloids Surf., A 257-258 (2005) 333-337.
[31] T. Nguyen, B. Pellegrin, C. Bernard, X. Gu, J.M. Gorham, P. Stutzman, et al., Fate of nanoparticles during life cycle of polymer nanocomposites, J. Phys. Conf. Ser. 304 (2011) 012060.
[32] X. Li, S. Luan, H. Yang, H. Shi, J. Zhao, J. Jin, et al., Surface modification of poly(styrene-b-(ethylene-co-butylene)-b-styrene) elastomer via photo-initiated graft polymerization of poly(ethylene glycol), Appl. Surf. Sci. 258 (2012) 2344-2349.
[33] J. Zhu, B. Birgisson, N. Kringos, Polymer modification of bitumen: Advances and challenges, Eur. Polym. J. 54 (2014) 18-38.
[34] H. Xingzhou, L. Zubo, Wavelength sensitivity of photooxidation of styrene-butadiene-styrene copolymer, Polym. Degrad. Stab. 48 (1995) 99-102.
[35] S.-S. Choi, H.-S. Chung, Y.-T. Joo, B.-K. Min, S.-H. Lee, Analysis of the whitening phenomenon of a thermoplastic elastomer article by UV weathering, Polym. Test. 30 (2011) 415-419.
[36] A.C. Areias, C. Ribeiro, V. Sencadas, N. Garcia-Giralt, A. Diez-Perez, J.L. Gómez Ribelles, et al., Influence of crystallinity and fiber orientation on hydrophobicity and biological response of poly(l-lactide) electrospun mats, Soft Matter 8 (2012) 5818-5825.